

# StructAlign: Structured Cross-Modal Alignment for Continual Text-to-Video Retrieval

Shaokun Wang, Weili Guan, Jizhou Han, Jianlong Wu, Yupeng Hu, Liqiang Nie

Harbin Institute of Technology (Shenzhen), Xi'an Jiaotong University, Shandong University

wangshaokun@hit.edu.cn, honeyguan@gmail.com, jizhou-han@stu.xjtu.edu.cn

wujianlong@hit.edu.cn, huyupeng@sdu.edu.cn, nieliqiang@gmail.com

## Abstract

*Continual Text-to-Video Retrieval (CTVR) is a challenging multimodal continual learning setting, where models must incrementally learn new semantic categories while maintaining accurate text-video alignment for previously learned ones, thus making it particularly prone to catastrophic forgetting. A key challenge in CTVR is feature drift, which manifests in two forms: intra-modal feature drift caused by continual learning within each modality, and non-cooperative feature drift across modalities that leads to modality misalignment. To mitigate these issues, we propose StructAlign, a structured cross-modal alignment method for CTVR. First, StructAlign introduces a simplex Equiangular Tight Frame (ETF) geometry as a unified geometric prior to mitigate modality misalignment. Building upon this geometric prior, we design a cross-modal ETF alignment loss that aligns text and video features with category-level ETF prototypes, encouraging the learned representations to form an approximate simplex ETF geometry. In addition, to suppress intra-modal feature drift, we design a Cross-modal Relation Preserving loss, which leverages complementary modalities to preserve cross-modal similarity relations, providing stable relational supervision for feature updates. By jointly addressing non-cooperative feature drift across modalities and intra-modal feature drift, StructAlign effectively alleviates catastrophic forgetting in CTVR. Extensive experiments on benchmark datasets demonstrate that our method consistently outperforms state-of-the-art continual retrieval approaches.*

## 1. Introduction

Continual Learning (CL), also referred to as Lifelong or Incremental Learning, aims to enable models to continuously acquire new knowledge from a stream of tasks while retaining previously learned information. Early studies on CL have primarily focused on single-modality settings,

such as image classification [28] and object detection [46]. Recently, CL has been extended to more complex and practically relevant multimodal tasks, including Image-Text Retrieval [65], Visual Question Answering [7, 73], and Text-to-Video Retrieval [76]. In these Multimodal Continual Learning (MCL) settings, models are required to process multiple modalities with separate or weakly coupled encoders, while continuously adapting to new tasks. This characteristic fundamentally differentiates MCL from its single-modality counterpart and makes it particularly vulnerable to catastrophic forgetting.

A primary cause of catastrophic forgetting is *feature drift*, as illustrated in Fig. 1(a), where strong data-fitting objectives drive feature representations to shift toward new tasks, gradually deviating from those learned for previous ones. In MCL, feature drift manifests in two forms. The first is *intra-modal feature drift*, where features within each individual modality evolve as the model adapts to new tasks. More critically, MCL introduces an additional challenge: *modality misalignment*, which arises from *non-cooperative feature drift* across modalities. Since different modalities are typically encoded by independent encoders, gradients induced by new tasks update these encoders unevenly and asynchronously during continual learning. As a result, features from different modalities may drift in different directions and with different magnitudes, gradually breaking the cross-modal alignment established on previous tasks.

This issue is particularly pronounced in text-to-video retrieval scenarios. As shown in Fig. 1(b), new tasks often contain novel visual content or temporal patterns, which strongly influence the video encoder and drive its feature space toward the new task distribution. In contrast, the text encoder usually receives weaker and less informative supervision, leading to relatively minor changes in its feature space. Such non-cooperative feature drift disrupts the shared feature space, causing semantically matched text and video features from previous tasks to become misaligned and resulting in severe performance degradation.

Motivated by these challenges, we study a novel and

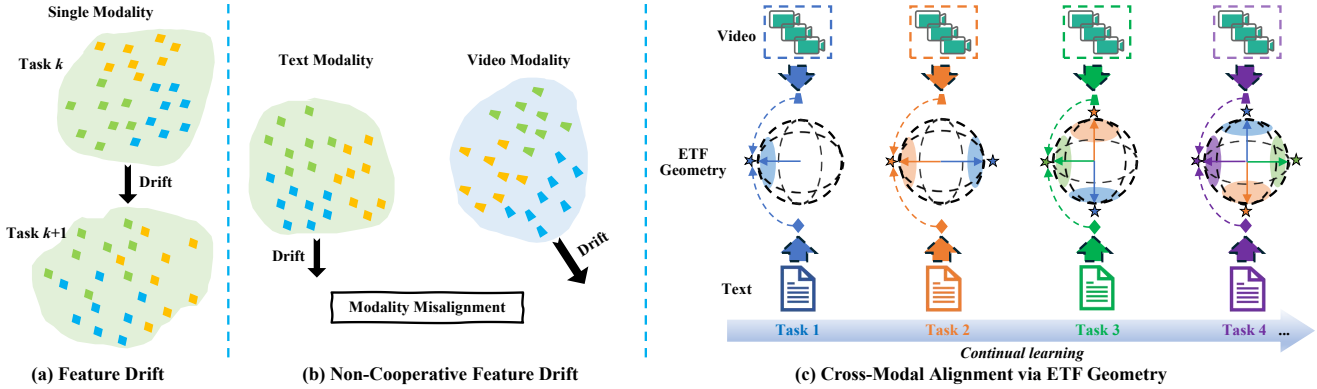


Figure 1. (a) In continual learning, feature drift refers to the phenomenon where feature representations shift toward new tasks, gradually deviating from feature representations learned for previous tasks. (b) In multimodal continual learning, features from different modalities tend to drift in a non-cooperative manner, which ultimately results in modality misalignment. (c) Our StructAlign adopts a simplex ETF geometry as a unified geometric prior to mitigate modality misalignment during multimodal continual learning.

practically relevant MCL setting: *Continual Text-to-Video Retrieval (CTVR)*, which was first introduced in [76]. CTVR requires models to preserve fine-grained cross-modal alignment while continuously adapting to new categories. Consequently, it amplifies both intra-modal feature drift and non-cooperative feature drift across modalities, making catastrophic forgetting particularly severe in this setting.

In this paper, we propose StructAlign, a structured cross-modal alignment method for CTVR. To address non-cooperative feature drift across modalities, we introduce a simplex Equiangular Tight Frame [39] (ETF) geometry as a unified geometric prior. This prior organizes multimodal representations in a shared feature space, as shown in Fig. 1(c). Based on this, we design a cross-modal ETF alignment loss that explicitly aligns text and video features with their corresponding ETF prototypes, encouraging the learned features to form an approximate simplex ETF geometry. By enforcing a well-separated category-level geometry and consistent cross-modal prototypes, this loss effectively reduces modality misalignment during continual learning. Even with improved cross-modal alignment, intra-modal feature drift remains a major source of catastrophic forgetting. To address this, we introduce a Cross-modal Relation Preserving (CRP) loss that leverages complementary modalities to preserve cross-modal similarity relations under the ETF-induced category geometry, thereby constraining intra-modal feature updates. Unlike conventional relational distillation methods designed for single-modality settings, CRP exploits cross-modal similarity relations as stable relational supervision, effectively regularizing intra-modal feature drift. By jointly addressing non-cooperative feature drift across modalities and intra-modal feature drift, our method effectively alleviates catastrophic forgetting in CTVR.

Comprehensive experiments on benchmark datasets demonstrate the effectiveness and consistent advantages of the proposed method. In-depth analyses further show that the learned feature space approximates the ideal Simplex ETF geometry, yielding well-separated categories while maintaining concentrated yet diverse intra-category features. In summary, the main contributions are listed as follows:

- We propose StructAlign, a structured cross-modal alignment framework for CTVR, which explicitly models and mitigates catastrophic forgetting induced by both intra-modal feature drift and non-cooperative feature drift across modalities.
- We introduce a simplex ETF geometric prior together with a cross-modal ETF alignment loss to enforce a well-separated category-level structure in the shared embedding space. In addition, we design a cross-modal relation preserving loss that leverages cross-modal similarity relations to constrain intra-modal feature updates during continual learning.
- Extensive experiments on benchmark datasets demonstrate that StructAlign consistently outperforms state-of-the-art continual retrieval methods.

## 2. Related Work

### 2.1. Continual Learning

A range of methods has been proposed to address catastrophic forgetting in CL settings, which can be grouped into four categories: 1) Regularization-based approaches [6, 13, 20, 30, 49, 50, 60] introduce additional loss terms to preserve previously acquired knowledge and implicitly constrain feature drift; 2) Architecture-based approaches [34, 38, 64,

74] dynamically expand or prune the network to reallocate parameters, accommodating new tasks while retaining old knowledge; 3) Rehearsal-based approaches [1, 8, 21, 22, 31, 61] store a small set of representative exemplars from prior data and replay them during continual learning to mitigate forgetting; and 4) Pre-trained model-based approaches [25, 28, 43, 48, 56, 58, 59, 79] build upon large-scale pre-trained models and are often combined with Parameter-Efficient Tuning [32] (PET), achieving improvements in both forgetting resistance and overall performance. It should be noted that these four categories are not mutually exclusive. Many CL models [2, 20, 24, 40, 49, 53, 54, 80] adopt hybrid strategies that combine multiple approaches. Recently, increasing attention has been paid to MCL [7, 10, 27, 47, 65, 73, 76], yet most existing methods still largely inherit techniques developed for unimodal continual learning. However, MCL introduces challenges that go beyond a straightforward extension of unimodal CL, as complex interactions across modalities substantially exacerbate catastrophic forgetting [68]. In this paper, we propose StructAlign to mitigate modality misalignment caused by non-cooperative feature drift across modalities, a fundamental challenge in MCL.

## 2.2. Text-to-Video Retrieval

Text-to-Video Retrieval (T2VR) [9, 45, 57, 81] aims to retrieve video content that semantically matches a given textual query. Early approaches [3, 11, 14, 55] rely on pre-trained modality-specific experts to extract offline features, followed by various strategies for multi-modal alignment, such as feature fusion modules [4, 70], attention-based aggregation [17, 33], and cross-modal contrastive learning losses [35, 67]. With the advent of large-scale vision-language models like CLIP [41], recent methods [15, 16, 29, 37, 44, 51, 71, 72, 75] have demonstrated significantly improved performance, achieving more effective and generalizable text-video alignment. Early work, such as CLIP4Clip [36], pioneered the use of pre-trained CLIP models for text-to-video retrieval. Building on this paradigm, X-Pool [18] introduces a text-conditioned video pooling mechanism that leverages cross-modal attention to dynamically aggregate the most semantically relevant frames for a given textual query. CLIP-ViP [63] enhances CLIP’s video understanding capability by incorporating auxiliary image captions and a proxy-guided video attention mechanism. PIG [26] proposes a Hybrid-Tower CLIP-based architecture that combines the efficiency of two-tower models with the effectiveness of single-tower models. VIDEO-COLBERT [42] advances fine-grained retrieval by enabling token-level interactions through MeanMaxSim over spatial and spatio-temporal levels. Despite their success, almost all existing methods assume access to the full training data in a single stage and yield

models whose functionality remains fixed after training. In contrast, real-world scenarios involve a continual stream of text-video pairs from previously unseen categories, resulting in evolving data distributions. These challenges highlight the importance of studying CTVR.

## 2.3. Applications of Equiangular Tight Frame Geometry

An Equiangular Tight Frame (ETF) characterizes a highly symmetric and well-separated geometric configuration, in which category prototypes are uniformly distributed in the embedding space with equal pairwise angles. Such a structure has been shown to naturally emerge in well-trained classifiers, a phenomenon commonly referred to as Neural Collapse (NC) [39]. Recent studies have extended NC-inspired formulations to various domains, including imbalanced classification [78], federated learning [23], class-incremental learning [19, 66], and domain-incremental learning [52]. In this work, we take a step further by introducing an ETF-based geometric constraint into the CTVR setting for the first time. Our goal is not to force features to collapse to a single point, as such collapse would harm retrieval tasks that require fine-grained and instance-level discrimination. Instead, we exploit the category-level structural property of ETF as a geometric prior to organize the shared embedding space into well-separated semantic regions. This design enables stable and consistent cross-modal alignment across tasks, while preserving sufficient intra-category variability to support effective text-to-video retrieval.

## 3. Preliminary

**Problem Setting.** In CTVR, the retrieval model learns query-video pairs over  $K$  training tasks, including one base task and  $K-1$  incremental tasks. At the  $k$ -th task, only the current dataset  $D^k = \{(\mathbf{t}_i, \mathbf{v}_i)\}_{i=1}^{|D^k|}$  is available, where  $\mathbf{t}_i$  and  $\mathbf{v}_i$  denote the  $i$ -th text query and video, respectively. Each video consists of  $M$  frames. Let  $\mathcal{Y}^k$  represent the set of new categories introduced in task  $k$ . These sets are disjoint across tasks, ensuring  $\forall i, j, \mathcal{Y}^i \cap \mathcal{Y}^j = \emptyset$ . The model parameterized by  $\theta$  is sequentially trained on  $D^1, D^2, \dots, D^K$ , and after learning from  $D^k$ , it is evaluated on all encountered categories  $\mathcal{Y}^{1:k} = \mathcal{Y}^1 \cup \mathcal{Y}^2 \cup \dots \cup \mathcal{Y}^k$ . Given all seen test queries, the model retrieves the most relevant videos from all previously learned tasks.

**Framework Overview.** Our framework builds upon frozen text and visual encoders, and incorporates lightweight parameter-efficient adaptation modules to support continual learning, together with a frame-word similarity function for text-to-video retrieval.

Given a text query  $\mathbf{t}$ , we employ the CLIP [41] Text

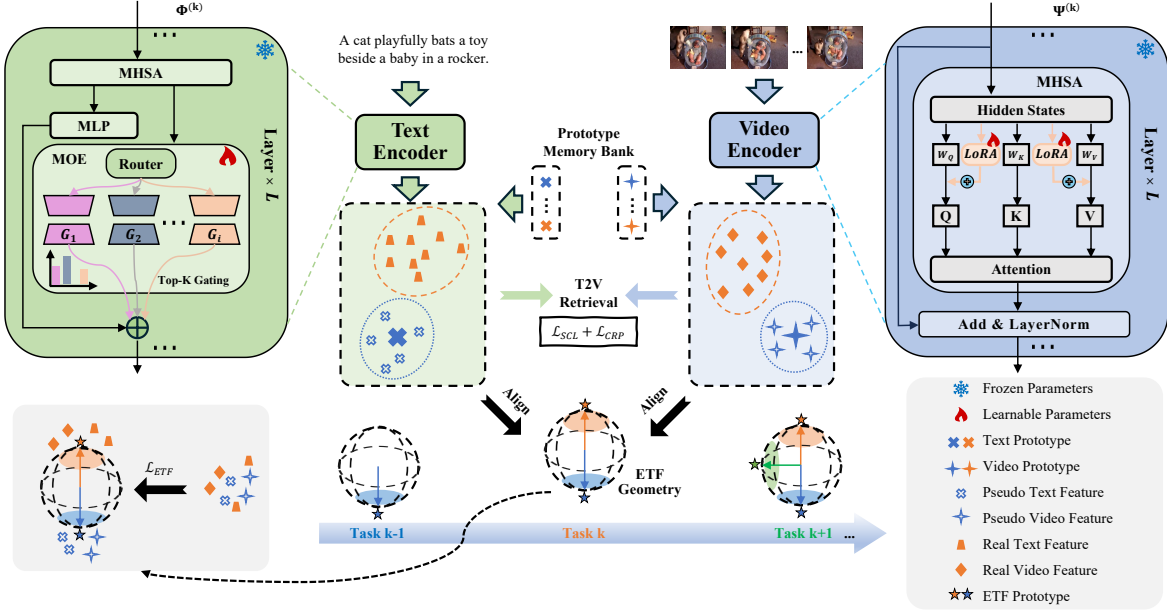


Figure 2. The overview of StructAlign. Based on a simplex ETF geometric prior, StructAlign explicitly aligns both real features from the current task and pseudo features from previous tasks with their corresponding ETF prototypes via a cross-modal ETF alignment loss  $\mathcal{L}_{ETF}$  (Sec. 4.2). Moreover, a cross-modal relation preserving loss  $\mathcal{L}_{CRP}$  is introduced to stabilize intra-modal feature updates by preserving cross-modal similarity relations under the ETF-induced geometry (Sec. 4.3 and Fig. 3).

**Encoder  $\Phi$  to extract word-level features:**

$$\Phi(\mathbf{t}) = \{\mathbf{w}^n\}_{n=1}^N, \quad (1)$$

where  $N$  denotes the length of the token sequence (the [EOS] token is omitted for brevity). To achieve a favorable plasticity-stability trade-off in continual learning, we freeze the parameters of the text encoder to preserve previously acquired knowledge, and inject a Mixture-of-Experts (MoE) module into the linear layers of each self-attention block to facilitate knowledge acquisition. Specifically, the MoE module employs a router  $\mathcal{R}(\cdot)$  to determine the contribution of each expert. Given an input  $x$ , the gating weights  $\mathbf{G} = \{G_i\}_{i=1}^I$  are computed as:

$$\mathbf{G} = \text{Softmax}(\text{Top-}k_e(\mathcal{R}(x))), \quad (2)$$

where  $\mathcal{R}(\cdot)$  projects  $x$  to a one-dimensional vector indicating the activation likelihood of each expert. The Top- $k_e(\cdot)$  selects the  $k_e$  most relevant experts while suppressing the remaining ones, and the  $\text{Softmax}(\cdot)$  function normalizes the selected weights to emphasize their relative contributions. Finally, the MoE output  $x'$  is obtained as a weighted combination of expert outputs:

$$x' = \sum_{i=1}^I G_i E_i(x), \quad (3)$$

where  $E_i(\cdot)$  denotes the  $i$ -th expert LoRA.

Given a video  $\mathbf{v}$  with  $M$  frames, we employ the CLIP [41] **Visual Encoder**  $\Psi$  to extract frame-level features:

$$\Psi(\mathbf{v}) = \{\mathbf{f}^m\}_{m=1}^M. \quad (4)$$

Analogous to the text encoder, we freeze all parameters of the visual encoder to preserve previously learned knowledge, and introduce LoRA modules to enable efficient task adaptation in a continual learning setting. Specifically, instead of modifying all self-attention projections, we inject LoRA modules only into the query and value projections of each self-attention block, while keeping the key projection unchanged. Concretely, given an input token sequence  $x$  at a self-attention layer, the original projection matrices  $W_Q, W_K, W_V \in \mathbb{R}^{D \times D}$  are frozen. We augment the query and value projections as:

$$\tilde{Q} = x(W_Q + \Delta W_Q), \quad \tilde{V} = x(W_V + \Delta W_V), \quad (5)$$

where  $\Delta W_Q = A_Q B_Q$ ,  $\Delta W_V = A_V B_V$ ,  $A_* \in \mathbb{R}^{D \times r}$ ,  $B_* \in \mathbb{R}^{r \times D}$ , and  $r \ll D$  denotes the rank of the LoRA.

**Frame-word Level Similarity.** The frame-word similarity measures the semantic alignment between a text sample  $\mathbf{t}_i$  and its corresponding video  $\mathbf{v}_j$  by aggregating fine-grained similarities between individual word and frame features:

$$\begin{aligned} \text{sim}(\mathbf{t}_i, \mathbf{v}_j) = & \frac{1}{2} \left( \frac{1}{N} \sum_{n=1}^N \max_{1 \leq m \leq M} \langle \mathbf{w}_i^n, \mathbf{f}_j^m \rangle \right. \\ & \left. + \frac{1}{M} \sum_{m=1}^M \max_{1 \leq n \leq N} \langle \mathbf{w}_i^n, \mathbf{f}_j^m \rangle \right) \end{aligned} \quad (6)$$

where  $N$  and  $M$  are the numbers of words and frames in the pair, respectively.  $\mathbf{w}_i^n \in \mathbb{R}^d$  and  $\mathbf{f}_j^m \in \mathbb{R}^d$  represent the features of the  $n$ -th word and the  $m$ -th frame, and  $\langle \mathbf{w}_i^n, \mathbf{f}_j^m \rangle$  denotes their cosine similarity. The first summation averages the maximum similarity that each word achieves with any frame, while the second summation performs the inverse operation over frames. The two terms are symmetrically averaged to ensure bidirectional consistency between text and video modalities.

## 4. Methodology

We first formulate an approximate Simplex ETF geometry to impose a category-level structure, and then introduce cross-modal ETF alignment and cross-modal relation preserving losses to address non-cooperative feature drift across modalities and intra-modal feature drift, respectively. Fig. 2 shows an overview of our method.

### 4.1. Approximate Simplex ETF Geometry for CTVR

We introduce an simplex ETF structure as a geometric prior to organize the shared feature space for CTVR. Instead of enforcing rigid feature collapse, it promotes a well-separated category-level geometry that supports cross-modal alignment while preserving intra-category variability. The term *approximate* emphasizes that ETF is employed as a soft geometric prior, rather than a strict convergence target.

**Definition of Simplex ETF Structure.** The joint feature space is organized around a set of  $C$  semantic prototypes, each corresponding to a distinct visual-textual concept. We denote these prototypes by  $P = [p_1, p_2, \dots, p_C] \in \mathbb{R}^{d \times C}$ , which are encouraged to form a simplex ETF configuration. In particular, an ideal reference ETF can be written as:

$$P^* = \sqrt{\frac{C}{C-1}} U \left( I_C - \frac{1}{C} \mathbf{1}_C \mathbf{1}_C^\top \right), \quad (7)$$

where  $U \in \mathbb{R}^{d \times C}$  is an orthogonal matrix satisfying  $U^\top U = I_C$ ,  $I_C$  is the  $C \times C$  identity matrix, and  $\mathbf{1}_C$  is a  $C$ -dimensional all-ones vector. We assume  $d \geq C$ , which holds in practice. Prototypes are  $\ell_2$ -normalized and regularized to remain close to this reference geometry. Their pairwise inner products follow the simplex ETF structure:

$$p_c^\top p_{c'} = \begin{cases} 1, & c = c', \\ -\frac{1}{C-1}, & c \neq c'. \end{cases} \quad (8)$$

The off-diagonal inner product  $-\frac{1}{C-1}$  characterizes the maximal equiangular configuration for  $C$  prototypes.

**ETF-Induced Geometric Properties.** With ETF-based organization and symmetric cross-modal contrastive learning (temperature  $\tau$ ), the joint feature space shows geometric properties that are beneficial for CTVR. For simplicity, the modality index is omitted when not explicitly required.

(P1) *Intra-category concentration.* Features belonging to the same semantic category are encouraged to concentrate around their corresponding prototype, without collapsing to a single point. Let  $\mu_{c,i}$  denote the feature of the  $i$ -th instance in category  $c$ , and  $\mu_c$  the category mean. The within-category covariance  $\Sigma_W^{(c)} = \text{Avg}\{(\mu_{c,i} - \mu_c)(\mu_{c,i} - \mu_c)^\top\}$  is constrained to remain bounded:  $\max_c \lambda_{\max}(\Sigma_W^{(c)}) \leq \eta$ , where  $\eta = O(e^{-1/\tau})$  controls the allowable intra-category variation.

(P2) *Inter-category equiangular separation.* After centering category means by the global mean  $\mu_G = \text{Avg}_{c,i}(\mu_{c,i})$ , the normalized category means  $\hat{\mu}_c = \frac{\mu_c - \mu_G}{\|\mu_c - \mu_G\|}$  are encouraged to align with the ETF prototypes. As a result, their pairwise inner products approximately follow the simplex ETF structure:

$$\hat{\mu}_c^\top \hat{\mu}_{c'} = \begin{cases} 1, & c = c', \\ -\frac{1}{C-1} + \varepsilon_{c,c'}, & c \neq c', \end{cases} \quad \text{with } |\varepsilon_{c,c'}| \leq \epsilon. \quad (9)$$

Here,  $\varepsilon_{c,c'}$  quantifies the deviation from the ideal equiangular configuration, and  $\epsilon = O(\sqrt{\eta} + e^{-1/\tau})$ .

(P3) *Cross-modal prototype consistency.* For each category  $c$ , the text and video features are aligned with the same ETF prototype  $p_c$ . Let  $\hat{\mu}_c^t$  and  $\hat{\mu}_c^v$  denote the normalized text and video category means, respectively. Their cross-modal discrepancy is quantified by  $\delta_c = 1 - \langle \hat{\mu}_c^t, \hat{\mu}_c^v \rangle$ , with  $\max_c \delta_c \leq \gamma$ , where  $\gamma = O(e^{-1/\tau})$ , and a smaller  $\gamma$  indicates stronger cross-modal geometric alignment.

**Discussion.** The bounded intra-category variation  $\eta$ , inter-category angular deviation  $\epsilon$ , and cross-modal discrepancy  $\gamma$  provide a unified characterization of the approximate Simplex ETF geometry. While the ETF prior specifies the desired category-level structure, symmetric cross-modal contrastive learning enforces these properties with controllable approximation errors.

### 4.2. Cross-modal ETF Alignment Loss

To realize the approximate Simplex ETF geometry, we design a cross-modal ETF alignment loss that explicitly enforces the alignment of text and video features with their corresponding ETF prototypes.

**Base Task.** Given a text-video pair  $(\mathbf{t}, \mathbf{v})$  with category label  $c \in [1, C]$ , let  $\Phi(\mathbf{t}) = \{\mathbf{w}^n\}_{n=1}^N$  and  $\Psi(\mathbf{v}) = \{\mathbf{f}^m\}_{m=1}^M$  denote token-level text features and frame-level video features. We first project token- and frame-level features into the shared ETF prototype space using modality-

specific MLPs:

$$\tilde{\mathbf{w}}^n = g_t(\mathbf{w}^n), \quad \tilde{\mathbf{f}}^m = g_v(\mathbf{f}^m), \quad (10)$$

where  $g_t(\cdot)$  and  $g_v(\cdot)$  map features to the same latent space as the ETF prototypes. Prototype-guided attention weights are computed as:

$$\alpha_n = \frac{\exp(\langle \tilde{\mathbf{w}}^n, p_c \rangle)}{\sum_{n'=1}^N \exp(\langle \tilde{\mathbf{w}}^{n'}, p_c \rangle)}, \quad \beta_m = \frac{\exp(\langle \tilde{\mathbf{f}}^m, p_c \rangle)}{\sum_{m'=1}^M \exp(\langle \tilde{\mathbf{f}}^{m'}, p_c \rangle)}, \quad (11)$$

where  $p_c$  denote the ETF prototype for category  $c$ . Modality-level representations are obtained via weighted pooling:

$$\bar{\mathbf{w}} = \sum_{n=1}^N \alpha_n \tilde{\mathbf{w}}^n, \quad \bar{\mathbf{f}} = \sum_{m=1}^M \beta_m \tilde{\mathbf{f}}^m. \quad (12)$$

The cross-modal ETF alignment loss for a mini-batch  $\mathcal{B}$  is:

$$\mathcal{L}_{ETF} = \frac{1}{|\mathcal{B}|} \sum_{(\bar{\mathbf{w}}, \bar{\mathbf{f}}, c) \in \mathcal{B}} \left[ (1 - \langle \hat{\mathbf{w}}, p_c \rangle) + (1 - \langle \hat{\mathbf{f}}, p_c \rangle) \right], \quad (13)$$

where  $\hat{\mathbf{w}} = \bar{\mathbf{w}} / \|\bar{\mathbf{w}}\|$  and  $\hat{\mathbf{f}} = \bar{\mathbf{f}} / \|\bar{\mathbf{f}}\|$ .

**Incremental Task.** In incremental tasks, text-video pairs from previously learned categories are no longer accessible. To preserve the embedding geometry and mitigate catastrophic forgetting, we leverage the learned modality-specific category prototypes (*i.e.* category means) as anchors. Let  $\hat{\mu}_c^t$  and  $\hat{\mu}_c^v$  denote the normalized text and video category means. For old categories, we synthesize pseudo features by adding Gaussian noise:

$$\tilde{\mathbf{w}}_c = \hat{\mu}_c^t + \epsilon_c^t, \quad \tilde{\mathbf{f}}_c = \hat{\mu}_c^v + \epsilon_c^v, \quad (14)$$

where  $\epsilon_c^t, \epsilon_c^v \sim \mathcal{N}(\mathbf{0}, \sigma^2)$ . These pseudo features are defined in the same feature space after  $g_t$  and  $g_v$ , ensuring geometric consistency with real samples.

Modality-level representations for current task samples are obtained in the same way as in the base task. We then enforce prototype alignment for both real and pseudo features using Eq. (13). This alignment ensures consistent geometric structure across incremental tasks and alleviates catastrophic forgetting without requiring access to old data.

### 4.3. Cross-modal Relation Preserving Loss

We have designed a cross-modal ETF alignment loss to alleviate non-cooperative feature drift across modalities by enforcing category-level geometric consistency. However, even with improved cross-modal alignment, intra-modal feature drift within each individual modality may still occur, which remains a major contributor to catastrophic forgetting. A direct solution would be to constrain features within each modality. However, existing approaches such as logit distillation [30] and relational distillation [20] are

primarily designed for single-modality settings or typically impose rigid instance-level constraints. Such constraints often overly restrict model plasticity, making them less suitable for CTVR.

To address intra-modal feature drift in a more semantically grounded manner, we propose a Cross-modal Relation Preserving (CRP) loss. Instead of directly constraining individual features, CRP leverages the complementary modality to construct cross-modal relations. The key insight is that while individual features may drift significantly during continual learning, the relative similarity relations across modalities are more stable. In particular, these relations are partially preserved by the ETF-based geometric prior and can therefore serve as effective anchors to regularize intra-modal feature updates.

Concretely, given a mini-batch of  $\mathcal{B}$  text-video pairs  $\{(\mathbf{t}_i, \mathbf{v}_i)\}_{i=1}^{\mathcal{B}}$ , we compute the cross-modal similarity matrices  $\mathbf{S}^k$  and  $\mathbf{S}^{k-1}$  under the current model  $\theta_k$  and the previous model  $\theta_{k-1}$ , respectively. For each text sample  $\mathbf{t}_i$ , its similarity to all video samples  $\{\mathbf{v}_j\}_{j=1}^{\mathcal{B}}$  under the current model is defined as:

$$\mathbf{S}_{i,j}^k = sim(\mathbf{t}_i, \mathbf{v}_j; \theta_k), \quad (15)$$

and analogously under the previous model as:

$$\mathbf{S}_{i,j}^{k-1} = sim(\mathbf{t}_i, \mathbf{v}_j; \theta_{k-1}), \quad (16)$$

where  $sim(\cdot, \cdot)$  is defined in Eq. (6).

By treating  $\mathbf{S}^{k-1}$  as a fixed relational anchor and encouraging  $\mathbf{S}^k$  to preserve its structure, as shown in Fig. 3, the CRP loss imposes a relation-level constraint on feature updates. Formally, it minimizes the Kullback-Leibler divergence between the softened similarity distributions, computed in a row-wise manner and averaged over the mini-batch:

$$\mathcal{L}_{CRP} = \frac{1}{\mathcal{B}} \sum_{i=1}^{\mathcal{B}} KL(\text{Softmax}(\mathbf{S}_{i,:}^{k-1} / \tau_2) \parallel \text{Softmax}(\mathbf{S}_{i,:}^k / \tau_2)), \quad (17)$$

where  $\mathbf{S}_{i,:}^k$  and  $\mathbf{S}_{i,:}^{k-1}$  denote the  $i$ -th row of the similarity matrix under model  $\theta_k$  and  $\theta_{k-1}$ , respectively.  $\mathcal{B}$  is the mini-batch size, and  $\tau_2$  is a temperature parameter.

### 4.4. Optimization Objective

We define a multi-part loss  $\mathcal{L}$  to simultaneously facilitate new knowledge acquisition and old knowledge preservation in CTVR:

$$\mathcal{L} = \begin{cases} \mathcal{L}_{SCL} + \lambda_1 \mathcal{L}_{ETF}, & k = 1, \\ \mathcal{L}_{SCL} + \lambda_1 \mathcal{L}_{ETF} + \lambda_2 \mathcal{L}_{CRP}, & k > 1, \end{cases} \quad (18)$$

where  $\mathcal{L}_{ETF}$  and  $\mathcal{L}_{CRP}$  are described in Eq. (13) and Eq. (17), respectively.  $\lambda_1$  and  $\lambda_2$  indicate the hyper-parameters

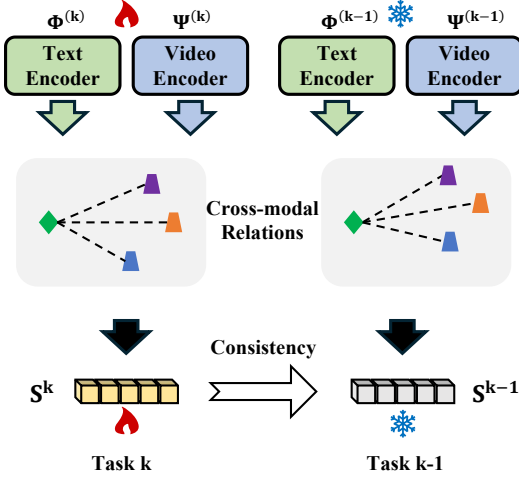


Figure 3. Illustration of the cross-modal relation preserving loss. By leveraging the complementary modality, cross-modal similarity matrices  $S^k$  and  $S^{k-1}$  are constructed under the current model  $\theta_k$  and the previous model  $\theta_{k-1}$ , respectively. Treating  $S^{k-1}$  as a fixed relational anchor, the current similarity matrix  $S^k$  is optimized to preserve its relational structure. For clarity, the text modality is shown as the auxiliary modality, while the formulation is symmetric across modalities.

to balance the contributions of the two losses. The retrieval loss  $\mathcal{L}_{SCL}$  is designed to pull semantically matched pairs closer in the shared feature space while pushing apart irrelevant ones. Specifically,  $\mathcal{L}_{SCL}$  is formulated as a symmetric contrastive loss consisting of text-to-video and video-to-text components:

$$\mathcal{L}_{t2v} = -\frac{1}{\mathcal{B}} \sum_{i=1}^{\mathcal{B}} \log \frac{\exp(sim(\mathbf{t}_i, \mathbf{v}_i)/\tau)}{\sum_{j=1}^{\mathcal{B}} \exp(sim(\mathbf{t}_i, \mathbf{v}_j)/\tau)}, \quad (19)$$

$$\mathcal{L}_{v2t} = -\frac{1}{\mathcal{B}} \sum_{i=1}^{\mathcal{B}} \log \frac{\exp(sim(\mathbf{t}_i, \mathbf{v}_i)/\tau)}{\sum_{j=1}^{\mathcal{B}} \exp(sim(\mathbf{t}_j, \mathbf{v}_i)/\tau)}, \quad (20)$$

$$\mathcal{L}_{SCL} = 1/2(\mathcal{L}_{v2t} + \mathcal{L}_{t2v}), \quad (21)$$

where  $|\mathcal{B}|$  denotes the mini-batch size,  $sim(\cdot, \cdot)$  represents the similarity function defined in Eq. (6), and  $\tau$  is a temperature parameter that controls the sharpness of the similarity distribution.

## 5. Experiments

In the following part of this section, we first provide the experimental setup, then present the evaluation results, and finally report ablation studies, hyper-parameter studies, and in-depth analysis. The experiments are designed to answer the following questions:

- **RQ1:** How does StructAlign perform compared to state-of-the-art CTVR methods?

- **RQ2:** How do the proposed components in StructAlign contribute to overall performance?

- **RQ3:** How do hyper-parameter settings affect StructAlign’s performance, and which settings yield the best results?

- **RQ4:** What inter-category and intra-category geometric structures emerge in the learned feature space under the proposed method?

Table 1. Datasets and continual learning protocol.

Dataset	#Category	Shot/Category	#Task
MSRVTT	20		16
ACTNET	200	16	$K=10, 20$

### 5.1. Experimental Setup

**Datasets.** We conduct extensive experiments on two widely used video-language benchmarks: **MSRVTT** [62] and **ACTNET** [5]. **MSRVTT** contains 10,000 short video clips, each paired with approximately 20 human-annotated textual descriptions. **ACTNET** consists of around 20,000 long and untrimmed videos covering 200 human activity categories collected from YouTube. We follow the CTVR protocol proposed in [76], where all categories are evenly partitioned into  $K$  tasks (with  $K = 10$  or 20), as shown in Table 1.

**Implementation Details.** The video and text encoders are initialized with the pre-trained CLIP ViT-B/32 [41], and all pre-trained weights are frozen during training. StructAlign is implemented in PyTorch. It is trained on a single NVIDIA A100 Tensor Core GPU for 20 epochs with a batch size of 32. In the base task, the initial learning rate is set to  $2 \times 10^{-5}$ , while for incremental tasks, it is set to  $3 \times 10^{-6}$  for MSRVTT and  $6 \times 10^{-6}$  for ACTNET. All comparison methods use the same training samples. The hyper-parameters  $\lambda_1$  and  $\lambda_2$  are set to 0.1 and 10, respectively.

**Comparison Methods.** We compare our method with three categories of competitive baselines to comprehensively evaluate its effectiveness:

(1) **State-of-the-art CTVR method**, *i.e.* StableFusion [76], which represents the current leading solution;

(2) **Classical continual learning methods**, including LwF [30], VR-LwF [12], ZSCL [77], and MoE-Adapter [69], which are originally designed for single modality continual learning but can be adapted to the CTVR setting;

(3) **Representative text-video retrieval methods**, including CLIP4Clip [36], X-Pool [18], and CLIP-ViP [63],

Table 2. Comparison of method performance for CTVR on MSRVTT and ACTNET datasets with 10 and 20 tasks. The top two methods are highlighted in **bold** and underlined. The second row of each method reports the standard deviation over three runs.

Method	MSRVTT-10						MSRVTT-20						ACTNET-10						ACTNET-20					
	R@1↑	R@5↑	R@10↑	Med↓	Mean↓	BWF↓	R@1↑	R@5↑	R@10↑	Med↓	Mean↓	BWF↓	R@1↑	R@5↑	R@10↑	Med↓	Mean↓	BWF↓	R@1↑	R@5↑	R@10↑	Med↓	Mean↓	BWF↓
ZS CLIP [41]	22.14 ±0.00	41.24 ±0.00	51.34 ±0.00	10.00 ±0.00	117.48 ±0.00	0.00	22.14 ±0.00	41.24 ±0.00	51.34 ±0.00	10.00 ±0.00	117.48 ±0.00	0.00	14.89 ±0.00	34.97 ±0.00	47.78 ±0.00	12.00 ±0.00	84.02 ±0.00	0.00	14.89 ±0.00	34.97 ±0.00	47.78 ±0.00	12.00 ±0.00	84.02 ±0.00	0.00
CLIP4Clip [36]	23.57 ±0.37	44.76 ±0.24	54.48 ±0.61	8.00 ±0.00	80.23 ±1.32	0.61 ±0.37	21.79 ±0.20	42.13 ±0.30	52.52 ±0.35	9.00 ±0.47	86.07 ±0.46	1.02 ±0.46	17.85 ±0.06	41.05 ±0.88	54.88 ±0.33	9.47 ±0.58	54.97 ±0.82	0.75 ±0.08	17.07 ±0.09	39.96 ±0.57	53.43 ±0.45	9.47 ±0.16	47.38 ±0.41	0.22
X-Pool [18]	19.60 ±0.35	39.80 ±0.63	49.49 ±0.54	11.00 ±0.00	94.89 ±1.70	0.28 ±0.40	15.98 ±0.75	34.21 ±1.52	44.34 ±0.87	15.33 ±0.58	105.97 ±1.97	1.37 ±0.23	17.99 ±0.54	39.81 ±0.87	52.38 ±1.06	9.67 ±0.58	60.49 ±1.49	0.37 ±0.39	16.57 ±0.38	39.83 ±0.47	51.82 ±0.35	10.22 ±0.19	55.00 ±1.58	0.31 ±0.43
CLIP-ViT [63]	21.56 ±1.07	44.19 ±0.31	53.43 ±0.52	8.00 ±0.00	86.71 ±0.71	0.49 ±0.74	19.74 ±0.19	41.25 ±0.29	50.61 ±0.20	10.00 ±0.00	93.95 ±1.19	0.73 ±0.31	17.01 ±0.53	38.73 ±0.82	52.01 ±0.75	9.67 ±0.58	59.66 ±1.50	0.56 ±0.21	16.02 ±0.19	37.29 ±0.21	50.92 ±0.71	10.58 ±0.38	48.78 ±1.16	0.73 ±0.13
LwF [30]	23.85 ±0.09	45.30 ±0.26	55.68 ±0.32	7.33 ±0.58	76.46 ±0.44	1.68 ±0.59	22.06 ±0.44	42.77 ±1.33	52.69 ±0.91	9.00 ±1.00	85.27 ±3.99	1.65 ±0.72	17.56 ±0.12	40.18 ±0.20	53.67 ±0.41	9.00 ±0.86	55.33 ±1.86	0.63 ±0.42	16.36 ±0.31	40.14 ±0.46	53.29 ±0.42	9.44 ±0.46	45.94 ±2.22	0.93 ±0.14
VR-LwF [12]	24.49 ±0.20	45.59 ±1.14	55.45 ±0.89	7.33 ±0.58	74.89 ±2.56	1.22 ±0.46	22.39 ±0.43	43.27 ±0.43	53.33 ±0.96	8.67 ±0.58	82.04 ±2.16	1.44 ±0.16	18.08 ±0.55	41.44 ±0.36	54.98 ±0.45	8.50 ±0.50	53.28 ±2.39	0.68 ±0.47	17.21 ±0.36	40.96 ±0.26	54.18 ±0.15	9.00 ±0.00	44.45 ±0.70	0.58 ±0.13
ZSCL [77]	23.99 ±0.44	45.15 ±0.33	54.77 ±0.24	8.00 ±0.00	79.69 ±0.95	0.10 ±0.78	21.47 ±0.77	41.61 ±0.87	52.05 ±0.92	9.33 ±0.58	88.45 ±6.38	0.91 ±0.33	17.67 ±0.55	41.05 ±0.47	54.05 ±0.15	9.00 ±0.00	55.74 ±0.19	0.35 ±0.45	16.83 ±0.17	38.90 ±0.55	52.07 ±0.31	9.33 ±0.58	65.03 ±1.59	0.70 ±0.08
MoE-Adapter [69]	22.92 ±0.09	42.76 ±0.24	52.11 ±0.32	9.00 ±0.38	105.70 ±0.58	0.14 ±0.59	22.70 ±0.44	41.96 ±1.33	51.82 ±0.91	9.00 ±1.00	112.86 ±3.99	0.14 ±0.72	16.63 ±0.12	37.29 ±0.20	50.36 ±0.41	10.33 ±0.86	70.49 ±1.86	0.15 ±0.42	15.77 ±0.31	36.27 ±0.46	49.32 ±0.42	11.00 ±0.25	77.65 ±2.22	0.01 ±0.14
TVR [63]+CL [12]	22.47 ±0.55	43.71 ±0.42	53.59 ±0.28	8.00 ±0.00	82.97 ±1.31	0.46 ±0.17	21.28 ±0.66	42.28 ±1.10	51.82 ±0.63	9.67 ±0.58	89.22 ±3.44	1.28 ±0.73	16.88 ±0.62	38.87 ±0.70	51.82 ±1.45	9.67 ±0.58	61.16 ±4.34	0.44 ±0.27	16.37 ±0.27	37.78 ±1.08	50.51 ±1.11	10.33 ±0.58	66.80 ±5.46	0.76 ±0.26
StableFusion [76]	25.87 ±0.33	45.91 ±0.03	56.03 ±0.64	7.00 ±0.64	74.70 ±0.00	-0.45 ±0.22	25.16 ±0.14	45.53 ±0.42	55.10 ±0.07	7.33 ±0.58	77.79 ±0.57	-0.70 ±0.40	18.21 ±0.23	40.45 ±0.34	53.94 ±0.34	9.00 ±0.63	56.14 ±0.63	-0.01 ±0.40	17.71 ±0.25	39.40 ±0.08	52.76 ±0.15	9.00 ±0.00	62.22 ±1.99	0.04 ±0.06
StructAlign	<b>25.98</b> ±0.20	<b>46.51</b> ±0.80	<b>57.13</b> ±0.31	<b>6.67</b> ±0.58	<b>73.27</b> ±1.08	<b>-0.47</b> ±0.07	<b>25.37</b> ±0.23	<b>45.94</b> ±0.17	<b>56.01</b> ±0.40	<b>7.00</b> ±0.65	<b>76.63</b> ±0.61	<b>-0.85</b> ±0.47	<b>18.26</b> ±0.20	<b>40.31</b> ±0.28	<b>54.68</b> ±0.36	<b>9.00</b> ±0.40	<b>48.82</b> ±0.36	<b>-0.68</b> ±0.40	<b>17.89</b> ±0.11	<b>39.69</b> ±0.30	<b>53.98</b> ±0.15	<b>9.00</b> ±0.00	<b>52.19</b> ±0.28	<b>-0.54</b> ±0.25
Upper Bound	25.86 ±0.67	48.34 ±0.25	58.96 ±0.12	6.00 ±0.00	65.10 ±1.09	-0.17 ±1.21	25.80 ±0.45	48.54 ±1.04	58.84 ±0.65	6.00 ±1.79	65.13 ±0.44	0.23 ±0.44	19.66 ±0.08	44.57 ±0.17	59.18 ±0.23	7.00 ±0.00	37.16 ±0.18	0.27 ±0.10	19.78 ±0.17	44.63 ±0.23	58.96 ±0.15	7.00 ±0.00	36.18 ±0.24	0.16 ±0.06

which reflect strong retrieval capabilities in standard non-incremental settings.

In addition, we report the Upper Bound performance, where the model is trained using the complete dataset from all tasks simultaneously, serving as an oracle reference to measure the performance gap induced by the continual learning setting.

**Evaluation Metrics.** We evaluate the proposed model using two categories of metrics. **(1) Retrieval Performance**

**Metrics.** To assess retrieval capability, we report Recall@1, Recall@5, Recall@10 (R@1, R@5, R@10), Median Rank (MedR), and Mean Rank (MeanR), where higher recall and lower ranking values indicate better performance. **(2) Continual Learning Metric.**

To quantify the model’s ability to retain previously learned knowledge while learning new tasks, we adopt the Backward Forgetting (BWF), which measures the average performance drop on earlier tasks. Specifically, when the model is trained up to task  $k$ , the BWF is defined as:  $BWF_k = \frac{1}{k-1} \sum_{i=1}^{k-1} (R_{i,i} - R_{k,i})$ , where  $R_{i,i}$  denotes the Recall@1 score on task  $i$  immediately after learning task  $i$ , and  $R_{k,i}$  represents its Recall@1 score after completing task  $k$ . A larger BWF implies more severe forgetting.

## 5.2. Comparison with State-of-the-Art Methods (RQ1)

We conduct comparison experiments on MSRVTT and ACTNET, where the incremental categories are divided equally into  $K$  (10 or 20) tasks.

**Evaluation on MSRVTT.** As shown in Table 2 and Fig. 4 (a)-(b), StructAlign obtains obvious advantages over the state-of-the-art CTVR methods and comparable performance compared to the Upper Bound: (1) it achieves the lowest Backward Forgetting and Mean Rank for all settings; (2) it achieves the highest Recall@5 and Recall@10 for the 10 and 20 task settings; and (3) it achieves comparable Recall@1 and Median Rank with the state-of-the-art CTVR method.

**Evaluation on ACTNET.** As we can see from Table 2 and Fig. 4 (c)-(d), StructAlign also achieves the best overall performance across all evaluated metrics on ACTNET. Specifically, (1) it attains the lowest Backward Forgetting across all settings; (2) it achieves the highest Recall@1 across all settings; and (3) it yields Recall@5, Recall@10, Mean Rank, and Median Rank comparable to those of the state-of-the-art CTVR method.

**Parameter Efficiency vs. Performance.** As shown in Fig. 5, we analyze the trade-off between retrieval performance and trainable parameters by comparing the average Recall@1 across four settings. Most existing methods, including CLIP4Clip, X-Pool, CLIP-ViT, LwF, VR-LwF, and ZSCL, update more than 150M parameters and achieve similar average Recall@1 scores, which fall within a narrow range of 17.5-20.5. Parameter-efficient methods such as MoE-Adapter and StableFusion substantially reduce the number of trainable parameters (to 59.8M and 46.8M, respectively) while maintaining competitive performance. Our StructAlign achieves the highest average Recall@1

Table 3. Ablation studies of StructAlign on MSRVTT and ACTNET, where the framework is described in Sec.3, *CETF* denotes the cross-modal ETF alignment loss based on a simplex ETF structure, and  $\mathcal{L}_{CRP}$  denotes the cross-modal relation preserving loss.

Dataset	#Task	MSRVTT							ACTNET								
		10			20				10			20					
Metric		R@1↑	R@5↑	R@10↑	MeanR↓												
Framework		22.71	42.61	52.81	100.97	21.82	42.40	53.06	83.26	14.84	35.63	47.94	60.12	15.71	36.47	50.50	59.75
Framework + $\mathcal{L}_{CRP}$		24.65	45.28	55.69	77.28	23.71	44.61	54.08	79.67	16.78	38.05	51.67	53.32	17.07	38.66	52.78	54.08
Framework + <i>CETF</i>		24.98	45.72	56.32	75.45	24.62	45.12	55.33	79.51	17.16	39.11	53.78	51.68	17.00	39.14	53.65	54.98
StructAlign		<b>25.98</b>	<b>46.51</b>	<b>57.13</b>	<b>73.27</b>	<b>25.37</b>	<b>45.94</b>	<b>56.01</b>	<b>76.63</b>	<b>18.26</b>	<b>40.31</b>	<b>54.68</b>	<b>48.82</b>	<b>17.89</b>	<b>39.69</b>	<b>53.98</b>	<b>52.19</b>

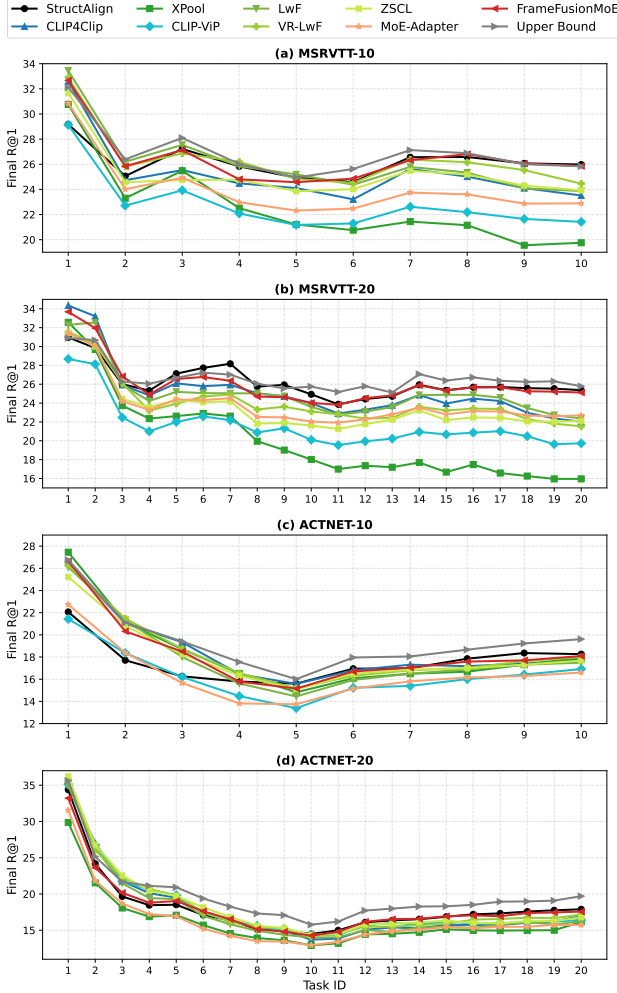


Figure 4. The comparison performance on MSRVTT (a)-(b) and ACTNET (c)-(d).

with only 33.9M trainable parameters, offering a more favorable balance between performance and parameter efficiency.

### 5.3. Ablation Studies (RQ2)

To investigate whether the performance gains are attributable to our proposed StructAlign, we conduct com-

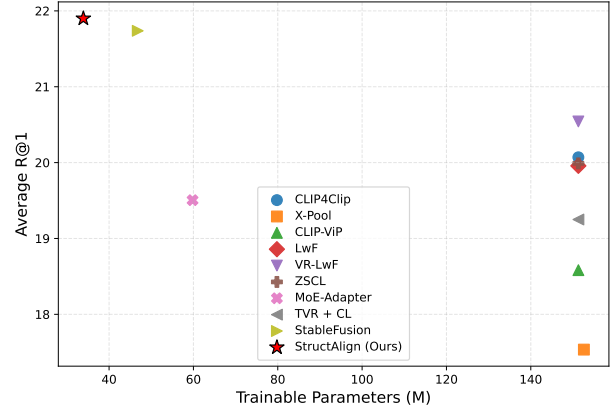


Figure 5. Trade-off between retrieval performance and trainable Parameters.

prehensive ablation studies on MSRVTT and ACTNET under different task settings. As reported in Table 3, we draw the following conclusions: (1) introducing the cross-modal relation preserving loss  $\mathcal{L}_{CRP}$  consistently improves retrieval performance over the baseline framework on both datasets, indicating that preserving cross-modal similarity relations effectively suppresses intra-modal feature drift during continual learning; (2) incorporating the cross-modal ETF alignment module *CETF* further boosts performance, demonstrating that enforcing a simplex ETF geometric prior effectively mitigates non-cooperative feature drift and modality misalignment across incremental tasks; (3) when  $\mathcal{L}_{CRP}$  and *CETF* are jointly applied, **StructAlign** achieves the best overall performance, which suggests that the two components are complementary and mutually reinforcing in alleviating catastrophic forgetting in CTVR.

### 5.4. Hyper-parameter Studies (RQ3)

We conduct ablation studies on the hyper-parameters  $\lambda_1$  and  $\lambda_2$ . As shown in Fig. 6, for  $\lambda_1$ , a small value of 0.1 achieves the best overall performance on both MSRVTT-10 and ACTNET-10, whereas larger  $\lambda_1$  slightly decreases Recall metrics. For  $\lambda_2$ , moderate values around 10 result in the highest overall performance, while very small or very

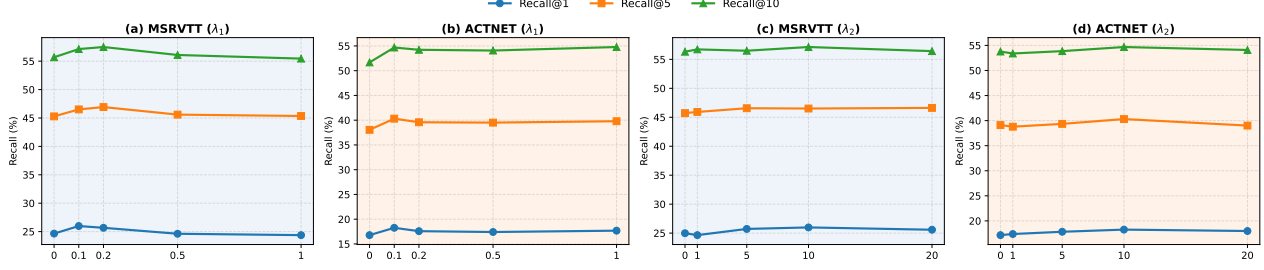


Figure 6. Hyper-parameter studies of  $\lambda_1$  and  $\lambda_2$  on MSRVTT and ACTNET.

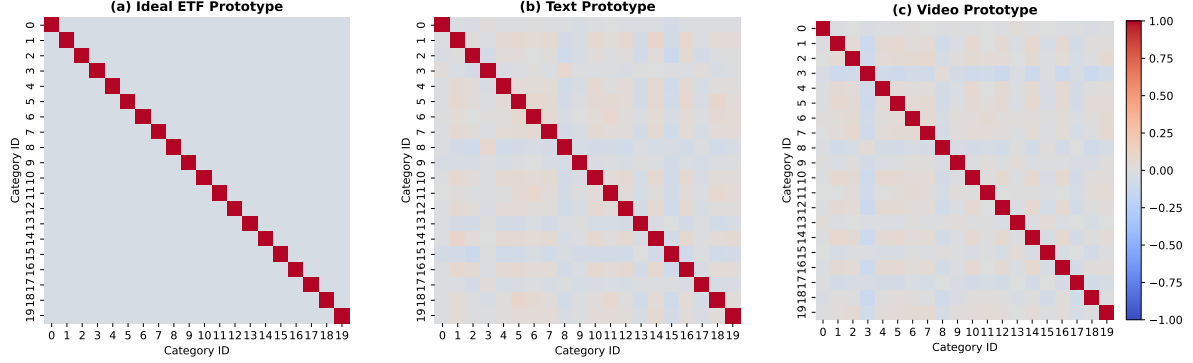


Figure 7. Pairwise cosine similarity matrices of (a) ideal Simplex ETF prototypes, (b) learned text prototypes, and (c) learned video prototypes.



Figure 8. Trend of MICD score over training steps.

large  $\lambda_2$  lead to sub-optimal performance. Based on these observations, we recommend the optimal hyper-parameter combination of  $\lambda_1 = 0.1$  and  $\lambda_2 = 10$ .

### 5.5. In-depth Analysis (RQ4)

To better understand how the proposed method organizes the feature space, we analyze both inter-category and intra-category geometric structures.

**Inter-Category Analysis.** Fig. 7 visualizes the pairwise similarity matrices of the ideal ETF prototypes and the learned text and video prototypes. As a geometric reference, the ideal ETF exhibits uniform negative off-diagonal similarities of  $-\frac{1}{C-1}$ , corresponding to equal angular separation among categories. Both text and video prototypes show approximately uniform inter-category simi-

larities and closely follow this equiangular pattern. This observation suggests that the learned representations exhibit well-separated category-level geometry under the proposed cross-modal ETF alignment loss. Moreover, the similarity patterns of text and video prototypes are consistent, suggesting that the two modalities share a similar category-level geometric organization.

**Intra-Category Analysis.** As shown in Fig. 8, we measure the concentration of intra-category feature distributions using the Mean Intra-Category Dispersion (MICD):

$$\text{MICD} = \frac{1}{C} \sum_{c=1}^C \frac{1}{|\mathcal{X}_c|(|\mathcal{X}_c|-1)} \sum_{\mathbf{x}_i, \mathbf{x}_j \in \mathcal{X}_c, i \neq j} \left(1 - \frac{\mathbf{x}_i \cdot \mathbf{x}_j}{\|\mathbf{x}_i\| \|\mathbf{x}_j\|}\right), \quad (22)$$

where  $C$  is the number of categories,  $|\mathcal{X}_c|$  is the number of samples in category  $c$ , and  $\mathbf{x}_i$  denotes the feature vector of the  $i$ -th sample. During training, MICD decreases from 0.3603 to 0.3369, indicating that features progressively concentrate around their category prototypes. Meanwhile, MICD remains strictly positive, confirming that features do not collapse and retain meaningful intra-category variability. This property is critical for text-to-video retrieval, as it preserves diverse instance-level semantics within each category, enabling fine-grained alignment between texts and videos.

## 6. Conclusion And Future Work

In this work, we propose StructAlign, a structured cross-modal alignment method for the CTVR task. Specifically, StructAlign relies on a simplex ETF geometry to impose a structured category-level organization in the shared feature space, which helps stabilize cross-modal alignment across tasks. Meanwhile, a cross-modal relation preserving loss complements this geometry by regulating intra-modal feature updates through cross-modal relational constraints. Extensive experiments on benchmark datasets demonstrate that StructAlign effectively alleviates catastrophic forgetting and consistently outperforms state-of-the-art methods in CTVR. A promising direction for future work is to extend the proposed geometric and relational constraints to broader multimodal continual learning scenarios, including more open and flexible retrieval settings.

## References

- [1] Hyojun Ahn, Jinseok Kwak, Suha Lim, and Hyunwoo J. Kim. Ss-il: Separated softmax for incremental learning. In *Proceedings of the IEEE/CVF International Conference on Computer Vision*, pages 844–853, 2021.
- [2] A. Ashok, K. J. Joseph, and V. N. Balasubramanian. Class-incremental learning with cross-space clustering and controlled transfer. In *European Conference on Computer Vision*, pages 105–122, 2022.
- [3] Max Bain, Arsha Nagrani, Gülcin Varol, and Andrew Zisserman. Frozen in time: A joint video and image encoder for end-to-end retrieval. In *Proceedings of the IEEE/CVF International Conference on Computer Vision*, pages 1708–1718, 2021.
- [4] Yi Bin, Wenhao Shi, Jipeng Zhang, Yujuan Ding, Yang Yang, and Heng Tao Shen. Non-autoregressive cross-modal coherence modelling. In *Proceedings of the ACM International Conference on Multimedia*, page 3253–3261, 2022.
- [5] Fabian Caba Heilbron, Victor Escorcia, Bernard Ghanem, and Juan Carlos Niebles. Activitynet: A large-scale video benchmark for human activity understanding. In *Proceedings of the IEEE Conference on Computer Vision and Pattern Recognition*, pages 961–970, 2015.
- [6] Massimo Caccia, Pau Rodriguez, Oleksiy Ostapenko, Fabrice Normandin, Min Lin, Alexandre Lacoste, Yoshua Bengio, and Jan-Willem van de Meent. Online fast adaptation and knowledge accumulation (osaka): A new approach to continual learning. *Advances in Neural Information Processing Systems*, 33:16532–16545, 2020.
- [7] Yuliang Cai and Mohammad Rostami. Clumo: Cluster-based modality fusion prompt for continual learning in visual question answering. *Journal of Artificial Intelligence Research*, 83, 2025.
- [8] Francisco M. Castro, Manuel J. Marín-Jiménez, Nicolas Guil, Cordelia Schmid, and Karteek Alahari. End-to-end incremental learning. In *European Conference on Computer Vision*, pages 233–248, 2018.
- [9] Shizhe Chen, Yida Zhao, Qin Jin, and Qi Wu. Fine-grained video-text retrieval with hierarchical graph reasoning. In *Proceedings of the IEEE/CVF Conference on Computer Vision and Pattern Recognition*, pages 10638–10647, 2020.
- [10] Shaoxu Cheng, Chiyuan He, Kailong Chen, Linfeng Xu, Hongliang Li, Fanman Meng, and Qingbo Wu. Vision-sensor attention based continual multimodal egocentric activity recognition. In *Proceedings of the IEEE International Conference on Acoustics, Speech and Signal Processing*, pages 6300–6304, 2024.
- [11] Ioana Croitoru, Simion-Vlad Bogolin, Marius Leordeanu, Hailin Jin, Andrew Zisserman, Samuel Albanie, and Yang Liu. Teachtext: Cross-modal generalized distillation for text-video retrieval. In *Proceedings of the IEEE/CVF International Conference on Computer Vision*, pages 11583–11593, 2021.
- [12] Yuxuan Ding, Lingqiao Liu, Chunna Tian, Jingyuan Yang, and Haoxuan Ding. Don’t stop learning: Towards continual learning for the clip model. *arXiv preprint arXiv:2207.09248*, 2022.
- [13] Arthur Douillard, Matthieu Cord, Charles Ollion, Thomas Robert, and Eduardo Valle. Podnet: Pooled outputs distillation for small-tasks incremental learning. In *European Conference on Computer Vision*, pages 86–102, 2020.
- [14] Alex Falcon, Giuseppe Serra, and Oswald Lanz. A feature-space multimodal data augmentation technique for text-video retrieval. In *Proceedings of the ACM International Conference on Multimedia*, pages 4385–4394, 2022.
- [15] Bo Fang, Wenhao Wu, Chang Liu, Yu Zhou, Yuxin Song, Weiping Wang, Xiangbo Shu, Xiangyang Ji, and Jingdong Wang. Uatvr: Uncertainty-adaptive text-video retrieval. In *Proceedings of the IEEE/CVF International Conference on Computer Vision*, pages 11583–11593, 2023.
- [16] Han Fang, Pengfei Xiong, Luhui Xu, and Wenhao Luo. Transferring image-clip to video-text retrieval via temporal relations. *IEEE Transactions on Multimedia*, 25:7772–7785, 2023.
- [17] Valentin Gabeur, Chen Sun, Karteek Alahari, and Cordelia Schmid. Multi-modal transformer for video retrieval. In *European Conference on Computer Vision*, pages 214–229, 2020.
- [18] Satya Krishna Gorti, Noël Vouitsis, Junwei Ma, Keyvan Golestan, Maksims Volkovs, Animesh Garg, and Guangwei Yu. X-pool: Cross-modal language-video attention for text-video retrieval. In *Proceedings of the IEEE/CVF Conference on Computer Vision and Pattern Recognition*, pages 5006–5015, 2022.
- [19] Yuhang He, Yingjie Chen, Yuhang Jin, Songlin Dong, Xing Wei, and Yihong Gong. Dyson: Dynamic feature space self-organization for online task-free class incremental learning. In *Proceedings of the IEEE/CVF Conference on Computer Vision and Pattern Recognition*, pages 23741–23751, 2024.
- [20] Saihui Hou, Xinyu Pan, Chen Change Loy, Zilei Wang, and Dahua Lin. Learning a unified classifier incrementally via rebalancing. In *Proceedings of the IEEE/CVF Conference on Computer Vision and Pattern Recognition*, pages 831–839, 2019.

[21] Qi Hu, Yizhou Gao, and Bo Cao. Curiosity-driven class-incremental learning via adaptive sample selection. *IEEE Transactions on Circuits and Systems for Video Technology*, 32(12):8660–8673, 2022.

[22] Xinyu Hu, Kaihua Tang, Chunyan Miao, Xian-Sheng Hua, and Hanwang Zhang. Distilling causal effect of data in class-incremental learning. In *Proceedings of the IEEE/CVF Conference on Computer Vision and Pattern Recognition*, pages 3957–3966, 2021.

[23] Chao Huang, Lingxi Xie, Yuhang Yang, Wenxuan Wang, Bin Lin, and Deng Cai. Neural collapse inspired federated learning with non-iid data. In *Proceedings of the IEEE/CVF Conference on Computer Vision and Pattern Recognition*, pages 21043–21052, 2023.

[24] K. J. Joseph, S. Khan, F. S. Khan, et al. Energy-based latent aligner for incremental learning. In *Proceedings of the IEEE/CVF Conference on Computer Vision and Pattern Recognition*, pages 7452–7461, 2022.

[25] D. Jung, D. Han, J. Bang, et al. Generating instance-level prompts for rehearsal-free continual learning. In *Proceedings of the IEEE/CVF International Conference on Computer Vision*, pages 11847–11857, 2023.

[26] Bangxiang Lan, Ruobing Xie, Ruixiang Zhao, Xingwu Sun, Zhanhui Kang, Gang Yang, and Xirong Li. Hybrid-tower: Fine-grained pseudo-query interaction and generation for text-to-video retrieval. In *Proceedings of the IEEE/CVF International Conference on Computer Vision*, pages 24497–24506, 2025.

[27] Mingrui Lao, Nan Pu, Yu Liu, Zhun Zhong, Erwin M. Bakker, Nicu Sebe, and Michael S. Lew. Multi-domain lifelong visual question answering via self-critical distillation. In *Proceedings of the ACM International Conference on Multimedia*, pages 4747–4758, 2023.

[28] Jiashuo Li, Shaokun Wang, Bo Qian, Yuhang He, Xing Wei, Qiang Wang, and Yihong Gong. Dynamic integration of task-specific adapters for class incremental learning. In *Proceedings of the IEEE/CVF Conference on Computer Vision and Pattern Recognition*, pages 30545–30555, 2025.

[29] Qian Li, Yucheng Zhou, Cheng Ji, Feihong Lu, Jianian Gong, Shangguang Wang, and Jianxin Li. Multi-modal inductive framework for text-video retrieval. In *Proceedings of the ACM International Conference on Multimedia*, page 2389–2398, 2024.

[30] Zhizhong Li and Derek Hoiem. Learning without forgetting. *IEEE Transactions on Pattern Analysis and Machine Intelligence*, 40(12):2935–2947, 2017.

[31] Hao Lin, Shikai Feng, Xiaobo Li, Guodong Xie, and Jing Huang. Anchor assisted experience replay for online class-incremental learning. *IEEE Transactions on Circuits and Systems for Video Technology*, 33(5):2217–2232, 2022.

[32] Peng Liu, Weizhen Yuan, Jing Fu, Weizhu Xiong, Xiang Jiang, Hiroaki Hayashi, and Graham Neubig. Pre-train, prompt, and predict: A systematic survey of prompting methods in natural language processing. *ACM Computing Surveys*, 55(9):1–35, 2023.

[33] Yang Liu, Samuel Albanie, Arsha Nagrani, and Andrew Zisserman. Use what you have: Video retrieval using representations from collaborative experts. In *Proceedings of the British Machine Vision Conference*, page 279, 2019.

[34] Yaoyao Liu, Bernt Schiele, and Qianru Sun. Adaptive aggregation networks for class-incremental learning. In *Proceedings of the IEEE/CVF Conference on Computer Vision and Pattern Recognition*, pages 2544–2553, 2021.

[35] Yuqi Liu, Pengfei Xiong, Luhui Xu, Shengming Cao, and Qin Jin. Ts2-net: Token shift and selection transformer for text-video retrieval. In *European Conference on Computer Vision*, pages 319–335, 2022.

[36] Huaishao Luo, Lei Ji, Ming Zhong, Yang Chen, Wen Lei, Nan Duan, and Tianrui Li. Clip4clip: An empirical study of clip for end to end video clip retrieval and captioning. *Neurocomputing*, 508:293–304, 2022.

[37] Yiwei Ma, Guohai Xu, Xiaoshuai Sun, Ming Yan, Ji Zhang, and Rongrong Ji. X-clip: End-to-end multi-grained contrastive learning for video-text retrieval. In *Proceedings of the ACM International Conference on Multimedia*, pages 638–647, 2022.

[38] Arun Mallya and Svetlana Lazebnik. Packnet: Adding multiple tasks to a single network by iterative pruning. In *Proceedings of the IEEE/CVF Conference on Computer Vision and Pattern Recognition*, pages 7765–7773, 2018.

[39] Vardan Papyan, XY Han, and David L Donoho. Prevalence of neural collapse during the terminal phase of deep learning training. *Proceedings of the National Academy of Sciences*, 117(40):24652–24663, 2020.

[40] A. Prabhu, P. H. S. Torr, and P. K. Dokania. Gdumb: A simple approach that questions our progress in continual learning. In *European Conference on Computer Vision*, pages 524–540, 2020.

[41] Alec Radford, Jong Wook Kim, Chris Hallacy, Aditya Ramesh, Gabriel Goh, Sandhini Agarwal, Girish Sastry, Amanda Askell, Pamela Mishkin, Jack Clark, et al. Learning transferable visual models from natural language supervision. In *International conference on machine learning*, pages 8748–8763, 2021.

[42] Arun Reddy, Alexander Martin, Eugene Yang, Andrew Yates, Kate Sanders, Kenton Murray, Reno Kriz, Celso M. De Melo, Benjamin Van Durme, and Rama Chellappa. Video-colbert: Contextualized late interaction for text-to-video retrieval. In *Proceedings of the IEEE/CVF Conference on Computer Vision and Pattern Recognition*, pages 19691–19701, 2025.

[43] J. S. Smith, L. Karlinsky, V. Gutta, et al. Coda-prompt: Continual decomposed attention-based prompting for rehearsal-free continual learning. In *Proceedings of the IEEE/CVF Conference on Computer Vision and Pattern Recognition*, pages 11909–11919, 2023.

[44] Xue Song, Jingjing Chen, and Yu-Gang Jiang. Relation triplet construction for cross-modal text-to-video retrieval. In *Proceedings of the ACM International Conference on Multimedia*, page 4759–4767, 2023.

[45] Xue Song, Jingjing Chen, Zuxuan Wu, and Yu-Gang Jiang. Spatial-temporal graphs for cross-modal text2video retrieval. *IEEE Transactions on Multimedia*, 24:2914–2923, 2022.

[46] Xiang Song, Yuhang He, Jingyuan Li, Qiang Wang, and Yihong Gong. Learning endogenous attention for

incremental object detection. In *IEEE/CVF Conference on Computer Vision and Pattern Recognition*, pages 30354–30364, 2025.

[47] Feng Sun, Hong Liu, Chao Yang, and Bin Fang. Multimodal continual learning using online dictionary updating. *IEEE Transactions on Cognitive and Developmental Systems*, 13(1):171–178, 2020.

[48] Y. M. Tang, Y. X. Peng, and W. S. Zheng. When prompt-based incremental learning does not meet strong pretraining. In *Proceedings of the IEEE/CVF International Conference on Computer Vision*, pages 1706–1716, 2023.

[49] Xiaoyu Tao, Xinyuan Chang, Xiaopeng Hong, Songlin Dong, Xing Wei, and Yihong Gong. Topology-preserving class-incremental learning. In *European Conference on Computer Vision*, pages 254–270, 2020.

[50] Xiaoyu Tao, Xiaopeng Hong, Xinyuan Chang, Songlin Dong, Xing Wei, and Yihong Gong. Bi-objective continual learning: Learning “new” while consolidating “known”. In *Proceedings of the AAAI Conference on Artificial Intelligence*, volume 34, pages 5989–5996, 2020.

[51] Kaibin Tian, Ruixiang Zhao, Zijie Xin, Bangxiang Lan, and Xirong Li. Holistic features are almost sufficient for text-to-video retrieval. In *Proceedings of the IEEE/CVF Conference on Computer Vision and Pattern Recognition*, pages 17138–17147, 2024.

[52] Qiang Wang, Yuhang He, Songlin Dong, Xiang Song, Jizhou Han, Haoyu Luo, and Yihong Gong. Dualcp: Rehearsal-free domain-incremental learning via dual-level concept prototype. In *Proceedings of the AAAI Conference on Artificial Intelligence*, pages 21198–21206, 2025.

[53] Shaokun Wang, Weiwei Shi, Songlin Dong, Xinyuan Gao, Xiang Song, and Yihong Gong. Semantic knowledge guided class-incremental learning. *IEEE Transactions on Circuits and Systems for Video Technology*, 33(10):5921–5931, 2023.

[54] Shaokun Wang, Weiwei Shi, Yuhang He, Yifan Yu, and Yihong Gong. Non-exemplar class-incremental learning via adaptive old class reconstruction. In *Proceedings of the ACM International Conference on Multimedia*, page 4524–4534, 2023.

[55] Xiaohan Wang, Linchao Zhu, and Yi Yang. T2vlad: Global-local sequence alignment for text-video retrieval. In *Proceedings of the IEEE/CVF Conference on Computer Vision and Pattern Recognition*, pages 5079–5088, 2021.

[56] Y. Wang, Z. Huang, and X. Hong. S-prompts learning with pre-trained transformers: An occam’s razor for domain incremental learning. *Advances in Neural Information Processing Systems*, 35:5682–5695, 2022.

[57] Ziyang Wang, Yi-Lin Sung, Feng Cheng, Gedas Bertasius, and Mohit Bansal. Unified coarse-to-fine alignment for video-text retrieval. In *Proceedings of the IEEE/CVF International Conference on Computer Vision*, pages 2804–2815, 2023.

[58] Z. Wang, Z. Zhang, S. Ebrahimi, et al. Dualprompt: Complementary prompting for rehearsal-free continual learning. In *European Conference on Computer Vision*, pages 631–648, 2022.

[59] Z. Wang, Z. Zhang, C. Y. Lee, et al. Learning to prompt for continual learning. In *Proceedings of the IEEE/CVF Conference on Computer Vision and Pattern Recognition*, pages 139–149, 2022.

[60] Guolei Wu, Shaogang Gong, and Pan Li. Striking a balance between stability and plasticity for class-incremental learning. In *Proceedings of the IEEE/CVF International Conference on Computer Vision*, pages 1124–1133, 2021.

[61] Yue Wu, Yinpeng Chen, Lijuan Wang, Yuancheng Ye, Zicheng Liu, Yandong Guo, and Yun Fu. Large scale incremental learning. In *Proceedings of the IEEE/CVF Conference on Computer Vision and Pattern Recognition*, pages 374–382, 2019.

[62] Jun Xu, Tao Mei, Ting Yao, and Yong Rui. Msr-vtt: A large video description dataset for bridging video and language. In *Proceedings of the IEEE Conference on Computer Vision and Pattern Recognition*, pages 5288–5296, 2016.

[63] Hongwei Xue, Yuchong Sun, Bei Liu, Jianlong Fu, Ruihua Song, Houqiang Li, and Jiebo Luo. Clip-vip: Adapting pre-trained image-text model to video-language alignment. In *The International Conference on Learning Representations*, 2023.

[64] Shipeng Yan, Jie Xie, and Xuming He. Der: Dynamically expandable representation for class incremental learning. In *Proceedings of the IEEE/CVF Conference on Computer Vision and Pattern Recognition*, pages 3014–3023, 2021.

[65] Weicai Yan, Ye Wang, Wang Lin, Zirun Guo, Zhou Zhao, and Tao Jin. Low-rank prompt interaction for continual vision-language retrieval. In *Proceedings of the ACM International Conference on Multimedia*, page 8257–8266, 2024.

[66] Bo Yang, Ming Lin, Yifan Zhang, Bin Liu, Xiaodan Liang, Rongrong Ji, and Qixiang Ye. Dynamic support network for few-shot class incremental learning. *IEEE Transactions on Pattern Analysis and Machine Intelligence*, 2023.

[67] Jianwei Yang, Yonatan Bisk, and Jianfeng Gao. Taco: Token-aware cascade contrastive learning for video-text alignment. In *Proceedings of the IEEE/CVF International Conference on Computer Vision*, pages 11542–11552, 2021.

[68] Dianzhi Yu, Xinni Zhang, Yankai Chen, Aiwei Liu, Yifei Zhang, Philip S. Yu, and Irwin King. Recent advances of multimodal continual learning: A comprehensive survey. *arXiv preprint arXiv:2410.05352*, 2024.

[69] Jiazu Yu, Yunzhi Zhuge, Lu Zhang, Ping Hu, Dong Wang, Huchuan Lu, and You He. Boosting continual learning of vision-language models via mixture-of-experts adapters. In *Proceedings of the IEEE/CVF Conference on Computer Vision and Pattern Recognition*, pages 23219–23230, 2024.

[70] Youngjae Yu, Jongseok Kim, and Gunhee Kim. A joint sequence fusion model for video question answering and retrieval. In *European Conference on Computer Vision*, pages 471–487, 2018.

[71] Bingqing Zhang, Zhuo Cao, Heming Du, Yang Li, Xue Li, Jiajun Liu, and Sen Wang. Quantifying and narrowing the unknown: Interactive text-to-video retrieval via uncertainty minimization. In *Proceedings of the IEEE/CVF International Conference on Computer Vision*, pages 22120–22130, 2025.

[72] Haonan Zhang, Pengpeng Zeng, Lianli Gao, Jingkuan Song, and Heng Tao Shen. Mpt: Multi-grained prompt tuning for

text-video retrieval. In *Proceedings of the ACM International Conference on Multimedia*, page 1206–1214, 2024.

[73] Xi Zhang, Feifei Zhang, and Changsheng Xu. Vqacl: A novel visual question answering continual learning setting. In *Proceedings of the IEEE/CVF Conference on Computer Vision and Pattern Recognition*, page 19102–19112, 2023.

[74] Hanbin Zhao, Yanwei Fu, Ming Kang, Yu-Xiong Wang, and Yonggang Xu. Mgsvf: Multi-grained slow versus fast framework for few-shot class-incremental learning. *IEEE Transactions on Pattern Analysis and Machine Intelligence*, 46(3):1576–1588, 2024.

[75] Shuai Zhao, Linchao Zhu, Xiaohan Wang, and Yi Yang. Centerclip: Token clustering for efficient text-video retrieval. In *Proceedings of the International ACM SIGIR Conference on Research and Development in Information Retrieval*, pages 970–981, 2022.

[76] Zecheng Zhao, Zhi Chen, Zi Huang, Shazia Sadiq, and Tong Chen. Continual text-to-video retrieval with frame fusion and task-aware routing. In *Proceedings of the International ACM SIGIR Conference on Research and Development in Information Retrieval*, page 1011–1021, 2025.

[77] Zangwei Zheng, Mingyuan Ma, Kai Wang, Ziheng Qin, Xiangyu Yue, and Yang You. Preventing zero-shot transfer degradation in continual learning of vision-language models. In *Proceedings of the IEEE/CVF International Conference on Computer Vision*, pages 19125–19136, 2023.

[78] Zhun Zhong, Jingyun Cui, Yifan Yang, Xudong Wu, Xiaojuan Qi, Xiangyu Zhang, and Jiaya Jia. Understanding imbalanced semantic segmentation through neural collapse. In *Proceedings of the IEEE/CVF Conference on Computer Vision and Pattern Recognition*, pages 19038–19048, 2023.

[79] D. W. Zhou, H. L. Sun, H. J. Ye, et al. Expandable subspace ensemble for pre-trained model-based class-incremental learning. In *Proceedings of the IEEE/CVF Conference on Computer Vision and Pattern Recognition*, pages 23554–23564, 2024.

[80] D. W. Zhou, H. J. Ye, and D. C. Zhan. Co-transport for class-incremental learning. In *Proceedings of the ACM International Conference on Multimedia*, pages 1645–1654, 2021.

[81] Jinkuan Zhu, Pengpeng Zeng, Lianli Gao, Gongfu Li, Dongliang Liao, and Jingkuan Song. Complementarity-aware space learning for video-text retrieval. *IEEE Transactions on Circuits and Systems for Video Technology*, 33(8):4362–4374, 2023.